

Influence of taphonomy on histological evidence for vertebral pneumaticity in an Upper Cretaceous titanosaur from South America

Tito Aureliano ^{a, b, c, *}, Aline M. Ghilardi ^{b, c}, Julian C.G. Silva-Junior ^{d, e}, Agustín G. Martinelli ^f, Luiz Carlos Borges Ribeiro ^e, Thiago Marinho ^e, Marcelo A. Fernandes ^c, Fresia Ricardi-Branco ^a, P. Martin Sander ^g

^a Institute of Geosciences, University of Campinas, Campinas, Brazil

^b Department of Geology, Federal University of Rio Grande do Norte, Natal, Brazil

^c Laboratory of Paleocology and Paleochronology, Federal University of São Carlos, São Carlos, São Paulo State, Brazil

^d Laboratório de Paleontologia de Ribeirão Preto, Faculdade de Filosofia, Ciências e Letras de Ribeirão Preto, Universidade de São Paulo, Ribeirão Preto, São Paulo State, Brazil

^e Centro de Pesquisas Paleontológicas "Llewellyn Ivor Price", Universidade Federal do Triângulo Mineiro, Peirópolis, Uberaba, Minas Gerais State, Brazil

^f CONICET-Sección Paleontología de Vertebrados, Museo Argentino de Ciencias Naturales 'Bernardino Rivadavia', Av. Ángel Gallardo 470, Buenos Aires, C1405DJR, Argentina

^g Division of Paleontology, University of Bonn, Nussallee 8, 53115, Bonn, Germany

ARTICLE INFO

Article history:

Received 17 July 2019

Received in revised form

15 October 2019

Accepted in revised form 22 November 2019

Available online 28 November 2019

Keywords:

Pneumosteum

Diagenesis

Histology

Sauropoda

Tomography

ABSTRACT

There is a necessity to systematically sample taxa to enlighten our knowledge on the presence of histological correlates of avian-like air sacs among dinosaurs. This work expands the studies on the occurrence of pneumosteum in sauropods to the Brazilian lithostrotian titanosaur *Uberabatitan ribeiroi*. This confirms previous hypotheses on the insertion of an air sacs system on titanosaurian vertebrae based on external observation and CT-scans. We also highlight that diagenesis can obliterate traces of pneumosteal bone. Caution is required to have a good understanding of the diagenetic history of the studied specimens. This could avoid false negatives, especially when sampling pneumatic histological traces in stem taxa. Additionally, we describe a new workflow for manipulating CT-scan data using open-source software. The goal is to make this technology more accessible to research groups with limited funding and potentialize the achievement of more paleontological data.

© 2019 Elsevier Ltd. All rights reserved.

1. Introduction

Saurischian dinosaurs are model organisms for the understanding of evolutionary extremes (Sander et al., 2011; Aureliano et al., 2018; Xu et al., 2015; Cerda et al., 2012; Sander, 2013), ranging from the mechanical sustaining of extremely large sauropod bodies to the lightness and agility of derived theropods (Sander et al., 2011; Perry et al., 2009; Bates et al., 2010; Dyke et al., 2013). Their biomineralized remains indicate a diverse array of adaptations in response to environmental changes in deep

time. Accelerated dinosaurian metabolism is evidenced through long bone tissue deposition rates (Sander et al., 2011; Mitchell & Sander, 2014; Cerda et al., 2017; Curry Rogers & Kulik, 2018). However, that would imply in gigantothermal overheating in sauropods, at least in theory (Wedel, 2003; Perry et al., 2009; Sander et al., 2011). In order to revert this situation, one of the evolutionary innovations that appeared in this group was their highly effective respiratory capacity, part and parcel of which was a system of air sacs (i.e. diverticula projected from the lungs) that permeated the body cavities and certain bones (Wedel, 2003; Wedel, 2009; Lambertz et al., 2018). In sauropodomorphs, several macrostructures in the axial skeleton (eg. fossae, laminae, and certain foramina) have been indicated also as attachment evidence of those structures (Wedel, 2003; Wedel, 2007; Wedel, 2009; Wilson et al., 2011; Yates et al., 2012; Wilson, 2012). However, research on fossil pneumaticity before 2018 was limited to indirect evidence either from direct observation of structures or

* Corresponding author. Institute of Geosciences, University of Campinas, Campinas, Brazil.

E-mail address: aureliano.tito@gmail.com (T. Aureliano).

from their computed tomographies. Very few is known on the histological equivalents of pneumaticity: the pneumosteum (Lambertz et al., 2018). Only two non-avian taxa have been sampled since: the basal neosauropods *Europasaurus* and *Diplodocus* sp. (Lambertz et al., 2018). However, new data is needed to obtain a better understanding on which occasions such tissue might be preserved in the fossil record. Therefore, there is an urge to sample more taxa across strata, wider geographical locations, and distinct phylogenetic contexts.

The titanosaurs from the Upper Cretaceous Bauru Basin, Southeast Brazil, have the potential to provide more data on this matter. Not only because of the abundance of sauropod material and taxonomic diversity, but also for presenting distinct taphonomy across individuals, units and outcrops. In this paper, we sampled a posterior cervical vertebra of a young individual of the derived neosauropod *Uberabatitan ribeiroi* (Salgado & Carvalho, 2008; Silva Junior et al., 2019) from Serra da Galga Member of the Marília Formation, in southwestern Minas Gerais. A combination of computed tomography, petrography and histology was conducted to study pneumaticity in this taxon and the micropreservation of fossil tissue.

Additionally, here we present a novel workflow for the three-dimensional reconstruction of fossils from CT-scan slices using strictly multi-system open source softwares. The goal is to make this technology more accessible to other research groups with limited to no funding. Hopefully, this will potentialize the extraction of novel computed tomography paleontological data from these less privileged but highly competent teams.

2. Material and methods

Institutional abbreviations: CPPLIP, Centro de Pesquisas Paleontológicas “Llewellyn Ivor Price”, Universidade Federal do Triângulo Mineiro, Peirópolis, Uberaba, Minas Gerais, Brazil; HU-UFSCar, Hospital Universitário, Universidade Federal de São Carlos, São Carlos, São Paulo, Brazil; PVL, Paleovertebrate Collection, Instituto “Miguel Lillo”, San Miguel de Tucumán, Argentina; MCT, Museu de Ciências da Terra, Rio de Janeiro, Brazil.

2.1. Material

The studied specimen (CPPLIP-1024; Fig. 1) corresponds to a posterior cervical vertebra, deposited at the Centro de Pesquisas Paleontológicas “Llewellyn Ivor Price”, Universidade Federal do Triângulo Mineiro, Peirópolis, Brazil. It was found in the site known as “BR-050 153” by personnel of the CPPLIP and it was included in the description of Carvalho & Salgado (2008) and Silva Junior et al. (2019).

2.2. Anatomical terminology and measurements

Here we employ the nomenclature proposed by Wilson et al. (2011) for vertebral fossae; Wilson (2012) for laminae, and Wedel et al. (2000) and Wedel (2003, 2007) for pneumatic structures. The histological nomenclature used herein is in accordance with Padian & Lamm (2013). We also employ the terms anterior and posterior instead of cranial and caudal.

Anatomical Abbreviations: **c**, centrum; **cdf**, centrodiapophyseal fossa; **cpol**, centrodiapophyseal lamina; **nc**, neural center; **pcdl**, posterior centrodiapophyseal lamina; **po**, postzygapophysis; **podf**, postzygapophyseal centrodiapophyseal fossa; **podl**, postzygodiapophyseal lamina; **spof**, spinopostzygapophyseal fossa; **tpol**, intrapostzygapophyseal lamina.

2.3. Computer tomography acquisition

A CT-scan of the specimen was obtained using a Philips Diamond Select Brilliance CT 16-slice medical scanner with more than 200 slices and a voxel size of 0.75 mm at the HU-UFSCar.

2.4. A new workflow for three-dimensional reconstruction and refinement using free software

The medical program 3D Slicer v4.10.2 (Fedorov et al., 2012) was used to import DICOM slices and analyze the data. This is usually enough for imaging tomographic slices. However, depending on the taphonomical peculiarities of the specimen, further filters may be applied for visualization. For example, in

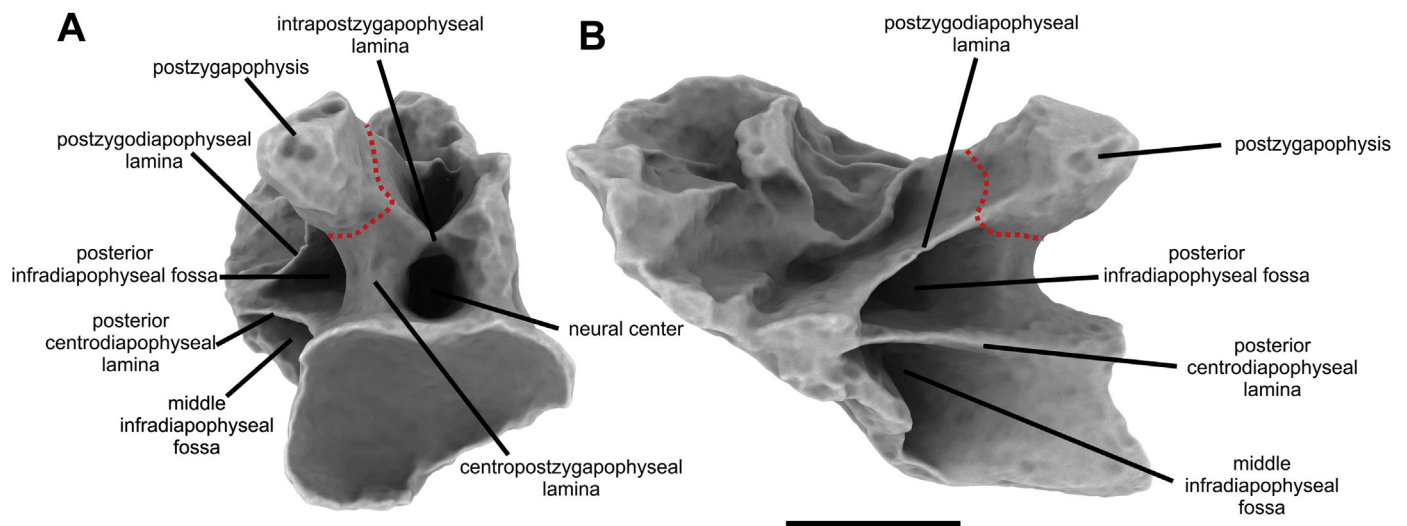


Fig. 1. Posterior cervical vertebra of the Upper Cretaceous Brazilian lithostrotian titanosaurian *Uberabatitan ribeiroi* (CPPLIP-1024). Three-dimensional reconstruction from CT-scan in proximal (A) and left lateral (B) views. Red line shows sampling plane. This photorealistic image table applies a novel technique of CT-scan data processing and refinement using open source software (see methods for details). **Abbreviations:** **c**, centrum; **cdf**, centrodiapophyseal fossa; **cpol**, centrodiapophyseal lamina; **nc**, neural center; **pcdl**, posterior centrodiapophyseal lamina; **po**, postzygapophysis; **podf**, postzygapophyseal centrodiapophyseal fossa; **podl**, postzygodiapophyseal lamina; **spof**, spinopostzygapophyseal fossa; **tpol**, intrapostzygapophyseal lamina. Scale bar = 100 mm. (For interpretation of the references to colour in this figure legend, the reader is referred to the Web version of this article.)

the vertebra of CPPLIP-1024 the contrast between sedimentary matrix and the camellate bone walls was very low. A volume filter using a preset for PET volume in rainbow colors was applied to highlight the pneumatic structures (Fig. 2). Afterwards, the volume is exported as a model at the desired format (eg. *.obj* or *.ply*). At this stage, one should use the model editor to cut out every unnecessary bias outside the specimen, such as eventual remnant tomography table pieces.

Structures such as sutures, fenestrae, fossae, and laminae are very relevant when describing characters. Therefore, figure plates

must be as clear as possible when highlighting those features. Sometimes, neither photograph of the fossil or the 3D model with 'metallic shade' make it clear enough to avoid misinterpretations. There is a further step in order to produce photorealistic figures highlighting the actual relevant data. We use another software, traditionally applied to the study of trace fossils: *CloudCompare* 2.9.1 (CloudCompare.2018). The model is imported in *CloudCompare* and one applies the Ambient Occlusion plugin (Tarini et al., 2003) to produce a photorealistic monochromatic with homogenized texture. Finally, one may take pictures at the desired views

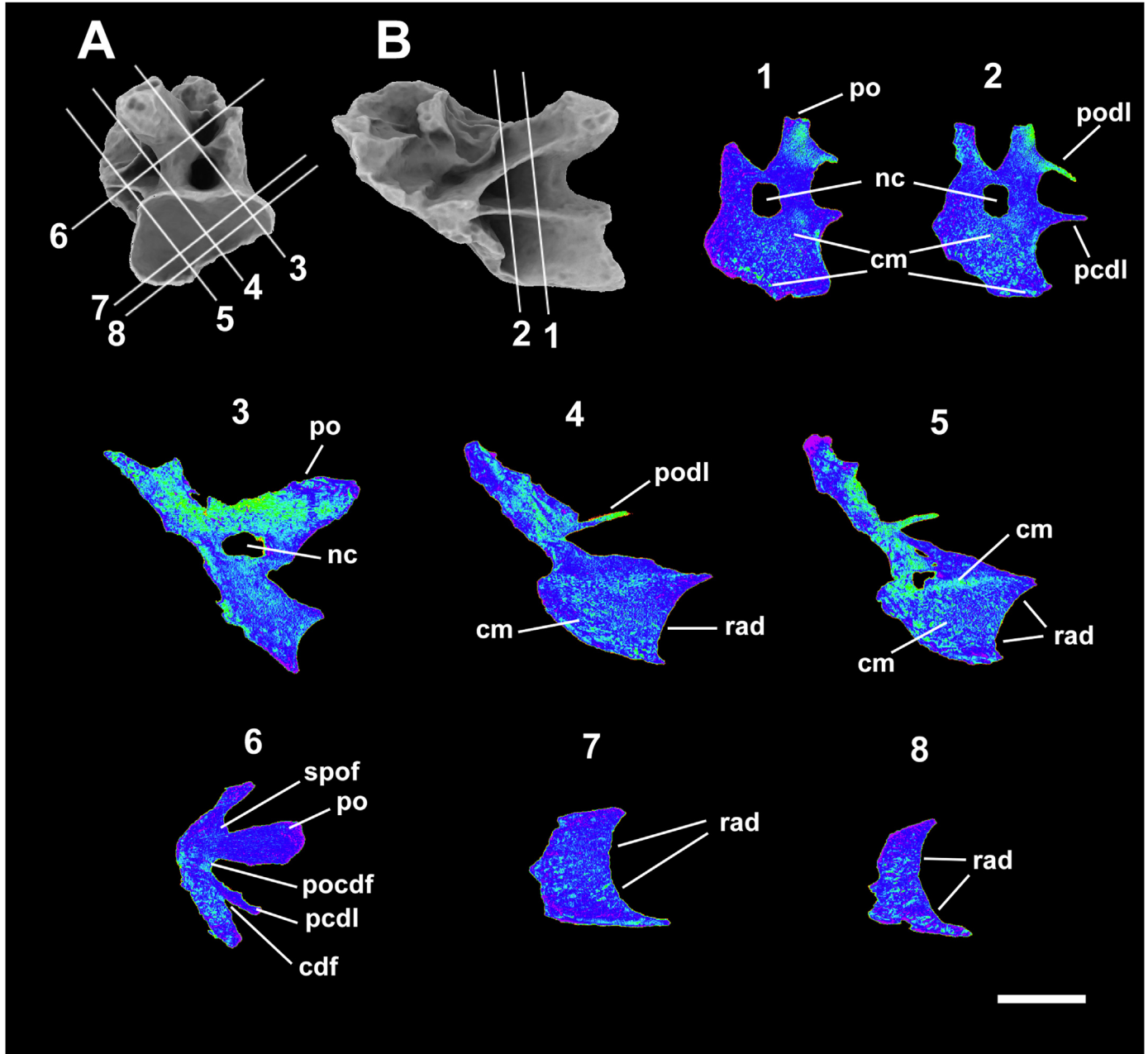


Fig. 2. Internal structures of the cervical vertebra of CPPLIP-1024 of *Uberabatitan ribeiroi*. Reconstructed three dimensional model in proximal (A) and lateral (B) views presenting inverted tangential CT-scan slices (1–8). Purple and darker blue indicate lower densities (eg. pneumatic cavities). Lighter blue and green demonstrate denser structures (eg. camellate bone). In this particular case, the latter might also indicate infilled sedimentary matrix and imaging artifacts. Excessively bright areas (eg. lighter green) are probably taphonomical artifacts (caused by localized diagenetic calcite percolation). **Abbreviations:** cm, camella; nc, neural canal; po, postzygapophysis; rad, radial camellae. Scale bar = 50 mm. (For interpretation of the references to colour in this figure legend, the reader is referred to the Web version of this article.)

within software and export as high-resolution images (see Fig. 1 for an example).

2.5. Bone histology

We followed the methodology presented by Lamm (2013) and Padian & Lamm (2013). The specimen was tomographed before sectioned. Pneumosteum is the histological correlates to the respiratory system, including the lungs, air sacs, and their diverticula (Lambertz et al., 2018). When pneumosteum tissue was first described, authors sampled the prezygapophysis of a cervical vertebra of the German basal neosauropod *Europasaurus holgeri* (Lambertz et al., 2018). In this work, we cross-sectioned the post-zygapophysis of the cervical vertebra of *Uberabatitan ribeiroi* in order to explore a different element. See Fig. 1 for the plane of section. Thin section was produced by following standard procedures (Lamm, 2013; Padian & Lamm, 2013) and grounded to a thickness of around 40–50 μm . Thin section was observed and photographed by using a petrographic ZEISS Axioscope microscope with coupled AxioCam MRC 5 camera, and imaging software ZEISS

Application Suite v.4.4. Pictures were corrected for brightness and contrast in Adobe Photoshop CC 20.0.1 and composite images were prepared in Corel Draw X6.

Specimen: CPPLIP-1024 (posterior cervical vertebra). The presence of other specimens up to three times larger (e.g. CPPLIP-1690) implies that CPPLIP-1024 was a young subadult individual (Silva Junior et al., 2019).

Locality and horizon: “BR-050 km 153” site, Serra da Galga area, about 25 km north of Uberaba city, Minas Gerais state of Brazil; Serra da Galga Member (da Fonseca Sampaio & Dal’Bó, 2017), Marília Formation (Salgado & Carvalho, 2008), Bauru Basin, Upper Cretaceous.

2.6. Diagnosis

This vertebra constitutes one of several specimens found on the type-locality of *Uberabatitan ribeiroi* (Salgado & Carvalho, 2008; Silva Junior et al., 2019). Only the left posterior portion is preserved (Fig. 1). It features a deep cotyle with subcircular shape and well-defined margins when seen in the posterior view. The volume

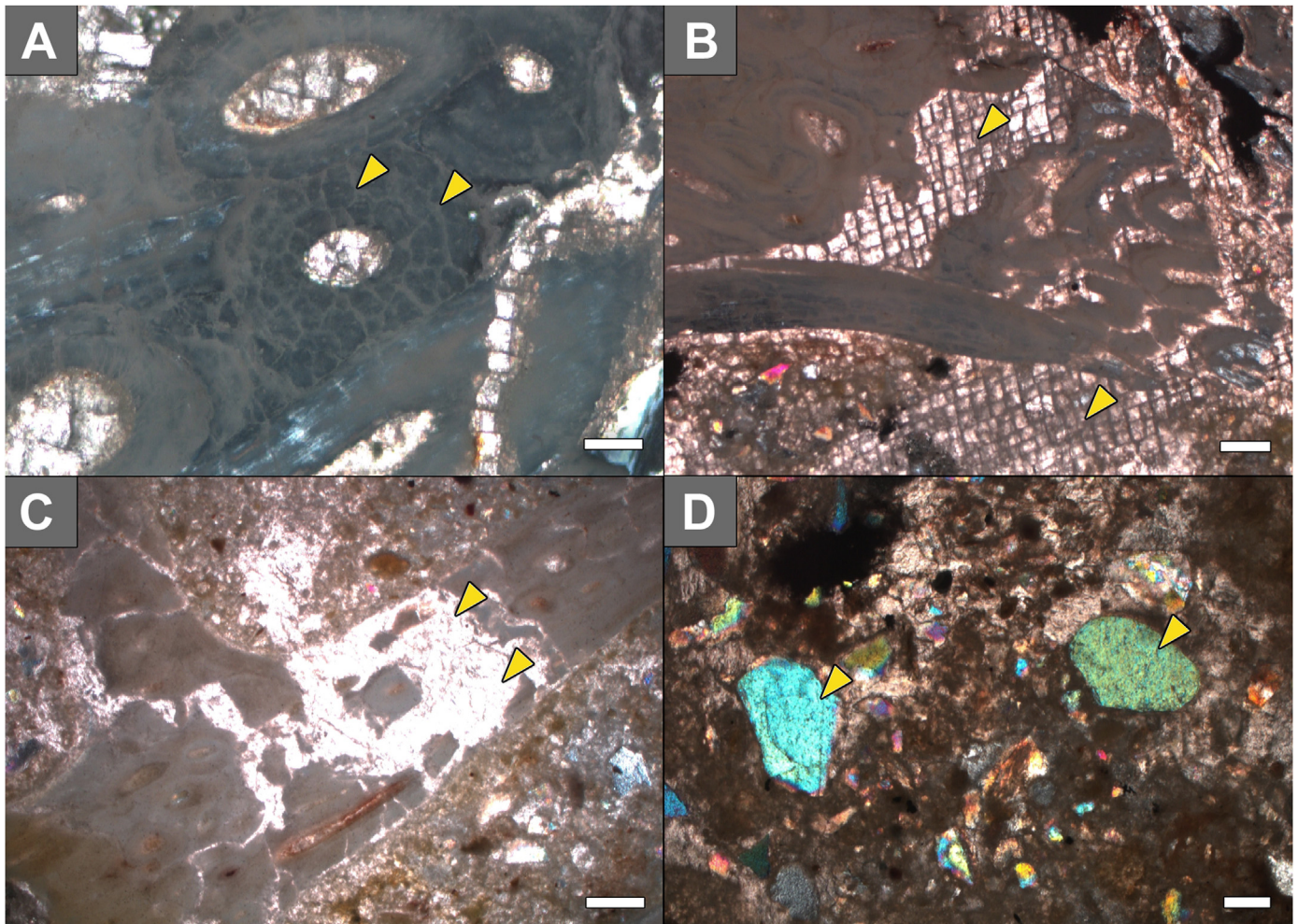


Fig. 3. Petrography picturing diagenetic features of CPPLIP-1024 of *Uberabatitan ribeiroi*. **A**, microscopic calcite cracks in trabeculae. **B**, Fractures infilled with diagenetic calcite. Note typical crystallographic acute twinning. **C**, localized trabeculae substituted and recrystallized by carbonate matrix. **D**, moderately unsorted subrounded to subangular quartz grains abound in a cavity. The high quartz birefringence shown in this photograph was caused because this thin section is higher than the petrographic standard (>32 μm). Polarized light under crossed nicols. Scale bar in **A**, **C**, **D** = 200 μm ; in **B** = 100 μm .

between the neural spine and the spinopostzygapophyseal fossa is not preserved. This latter fossa deepens until close to the neural center and is posteroventrally delimited by the intra-postzygapophyseal lamina. The postzygapophysis bears a large and flat articular facet and is connected with the centrum by a columnar centropostzygapophyseal lamina and with the neural spine by the eroded spinopostzygapophyseal lamina. On the lateral view, the postzygapophysis is connected to the eroded diapophysis by the compact postzygodiapophyseal lamina, which delimits the postzygapophyseal centrodiapophyseal fossa. This fossa excavates medially until close to the neural canal and is limited ventrally by the posterior centrodiapophyseal lamina. Foramina are absent throughout preserved volume.

3. Results

3.1. CT-scan

Tomography slices and the reconstructed three dimensional model allowed a successful observation of the internal pneumatic structures of *Uberabatitan ribeiroi* specimen CPPLIP-1024. The postzygapophysis is denser at the base and increases pneumaticity distally (Fig. 2.1–3, 6). It is also more pneumatized than the laminae. The middle infradiapophyseal fossa shows greater pneumatization than both laminae and postzygapophysis base (Fig. 2.6). In the neural center, camellae are smaller distally and increase inwards. Camellae follow slightly radial pattern within centrum distally, perpendicular to the cotyle internal surface (in lateral and ventral views; see Fig. 2.7,8). These are subhorizontally elongated throughout centrum (in lateral and ventral views; Fig. 2.4, 5, 7, 8).

3.2. Taphonomy and petrography

The vertebra preserves only its mid-posterior volume. This loss might have happened either during pre-burial transport. There are cracks all over the vertebral surface and internally to the microscopic level (Fig. 3A). These fractures are usually filled with diagenetic calcite. These are evidenced through minerals featuring high birefringence with rainbow aspect and typical crystallographic acute twinning (Fig. 3B). Calcite also occur as subangular grains amidst matrix. Localized areas of the trabeculae were substituted and recrystallized by carbonate matrix (Fig. 3C). There are also mineral grains composed of quartz, K-feldspar, and fractured hydroxyapatite camellate bone. Moderately unsorted subrounded quartz grains abound in every infilled cavity (Fig. 3D).

3.3. Histology

The postzygapophysis cross-section reveals a moderately preserved internal camellate pattern (Fig. 4). Bone walls present a conservative thickness of 1 mm (ranging between 0.5 and 2.0 mm). The camellate pockets vary greatly in size (from 1.5 to 7 mm wide) and shape, from subquadrangular to trapezoid forms. Smaller cavities are closer to the bone surface and get larger inwards.

The bone comprises regular trabeculae in most of its extension. Internally, camellate walls comprise tightly packed secondary lamellar bone in their longer axes. The intersection between chambers presents localized secondary osteons. Laminae (podl, cpol, tpol) feature secondary remodeling up to the cortical surface. About 95% of the entire microstructure was compromised by diagenetic calcite, giving a 'milky' texture covering most of the

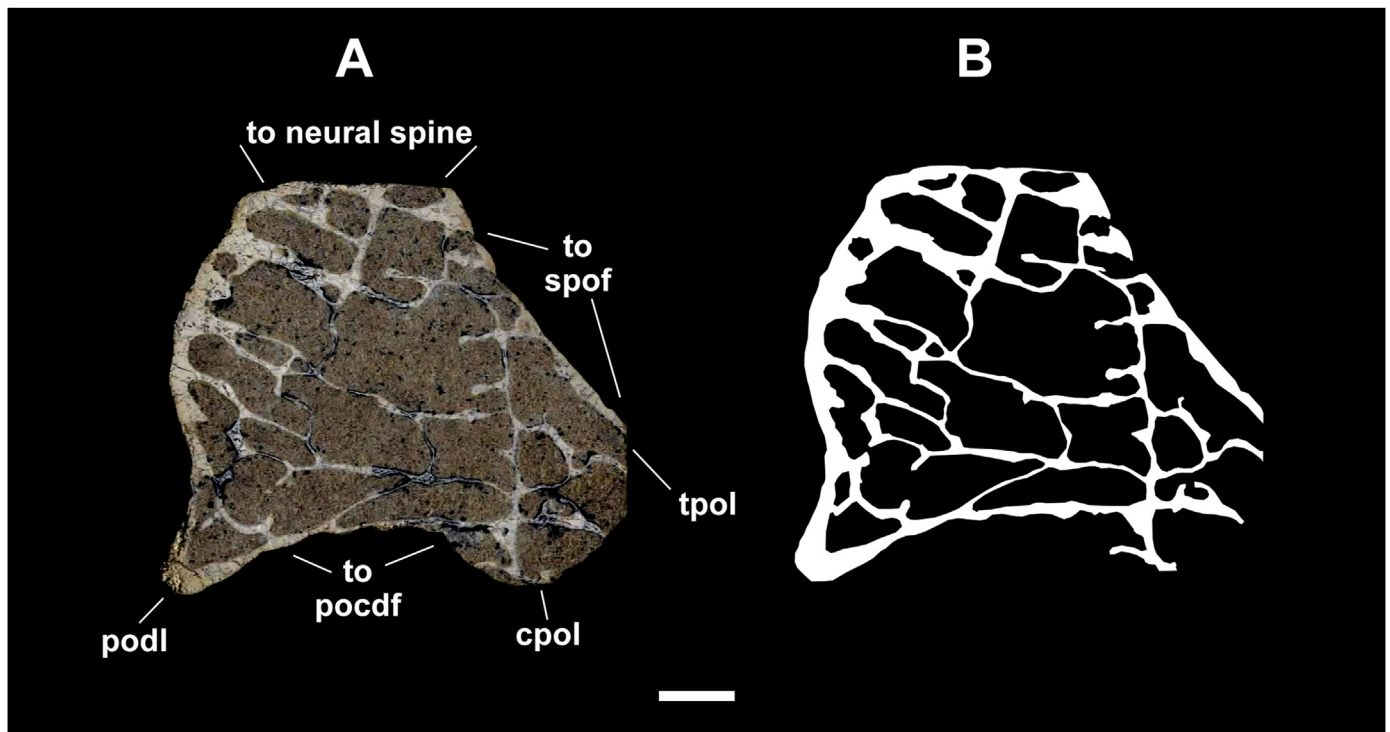
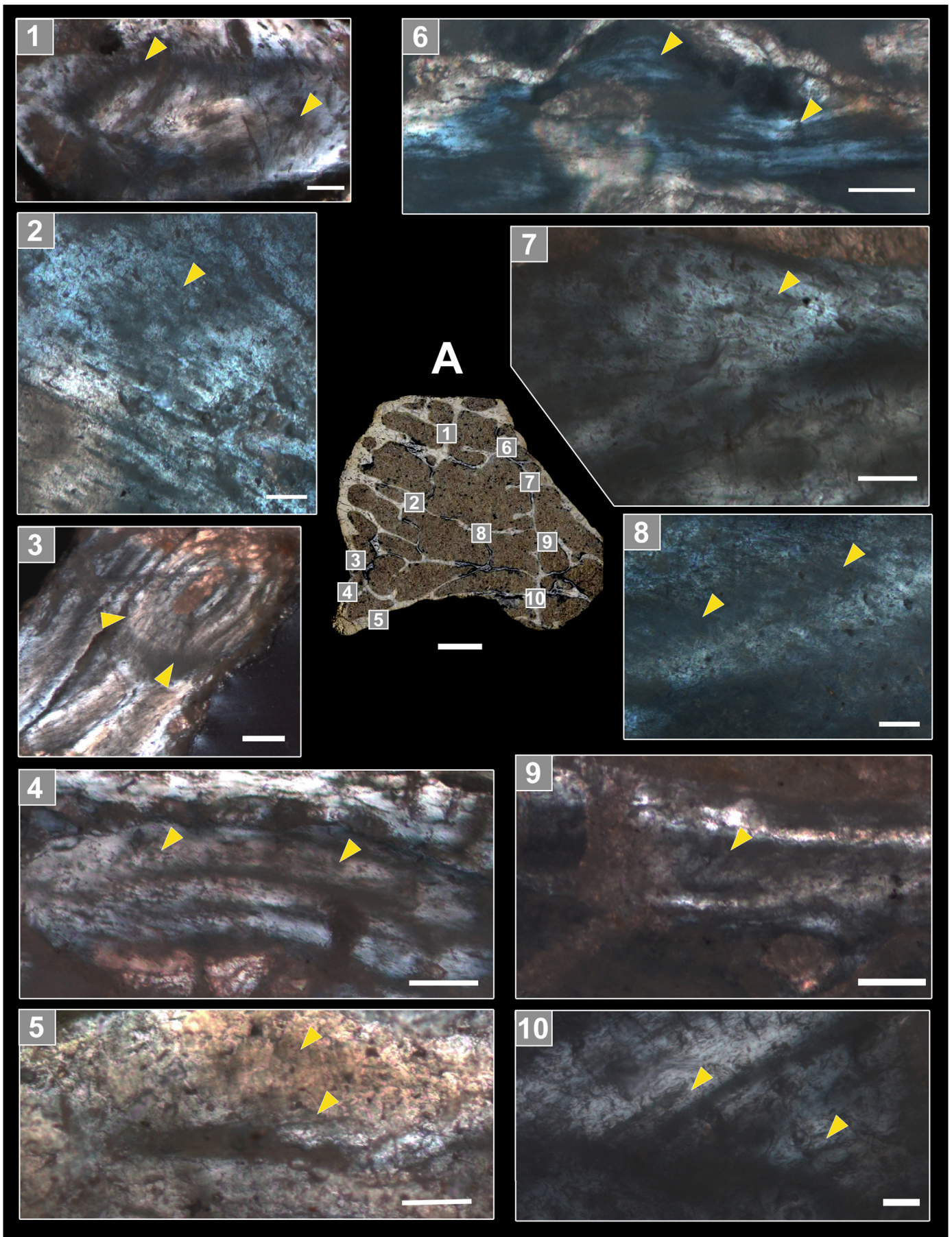


Fig. 4. Camellate bone structure in the postzygapophysis cross-section of *Uberabatitan ribeiroi* (CPPLIP-1024). **A**, photograph of the polished cross-section indicating laminae (cpol, podl, and tpol) and surfaces leading to fossae (pocdf, spof). The surface linked to the neural spine is eroded. **B**, manually delineated camellate bone walls from the cross-section. Note the majority of subquadrangular and subtrapezoidal shapes. Smaller cavities are closer to the bone surface. Scale bar = 10 mm.



observable areas. Even after these destructive events, there are isolated spots where pneumosteum has survived diagenetic destruction (Fig. 5). Except by the podl, pneumosteal tissue preservation was more common in interior camellae closer to the neural spine, the cpol, tpol, and in the surface to the spof. Pneumosteal tissue is recognized by and distinguished from the secondary lamellar trabecular tissues by presenting an undulose extinction and a densely packed fabric of tiny 'hair-like' fibers. The appearance of these resembles the asbestiform parallel fibrous aggregates of serpentines (Da Mommio, 2018). Nonetheless, pneumosteum present a smaller scale compared to serpentines. The eroded crenulated surface facing the pocdf, and the surrounding camellae, did not preserve any pneumosteum due to diagenetic destruction. However, some are preserved in loose trabeculae and primary tissue in the camella closer to the neural spine, spof. In the podl, there is pneumosteal tissue in both the external and internal surfaces of the lamina.

4. Discussion

There are several features in the *Uberabatitan ribeiroi* vertebra indicating attachment to pneumatic structures. Several laminae delineate large deep fossae in which diverticula anchored. Foramina are absent, however. This is probably because CPPLIP-1024 was a young individual and foramina develop later in ontogeny (Wedel, 2003; Wedel, 2007; Wedel, 2009). Nevertheless, Ct-scan images also reveal a complex array of smaller cavities that abound inside the centrum and in the postzygophysis. These internal pneumatic cavities are elongated posteriorly and slightly radial to the cotyle internal surface, similar to *Austroposeidon magnificus* cervicals (MCT 1628-R; Bandeira et al., 2016). The camellate fabric of CPPLIP-1024 shows a subquadrangular to subtrapezoidal shape. This is similar to the cervical of *Saltasaurus loricatus* (PVL 4017-214) and differs from the pattern seen in dorsals (eg. PVL 4017-47) and caudals (eg. PVL 4017-37) of the Argentinean taxon (Cerda et al., 2012). Dorsals and caudals present an even more chaotic array of camellae. Both *Saltasaurus* specimens from Cerda et al. (2012) belonged to adult individuals of approximately the same ontogenetic stage. Although not commented on by those authors, it is possible that the camellate architecture may indicate which air sacs system has influenced them. Therefore, further samples would contribute to solve questions about the pneumatization development along the axial skeleton (see Wedel, 2003). The similarities between the pattern across derived titanosaurs CPPLIP-1024 and PVL 4017-214 may indicate the influence of the cervical air sac system. However, further samples in more taxa are necessary to test this hypothesis.

Pneumatic structures are relevant in dinosauriform phylogeny (Wedel, 2006; O'Connor, 2006; Wedel, 2007; Yates et al., 2012). Pneumosteal tissue is indirect evidence of the contact of air-sac diverticula with the skeleton (Lambertz et al., 2018). Within non-avian dinosaurs, this tissue has been confirmed in the Jurassic neosauropods *Europasaurus holgeri* and *Diplodocus* sp.. We now report vertebral pneumosteum in the derived non-saltasaurine lithostrotian titanosaur *Uberabatitan ribeiroi*. In the spots with the best preservation, pneumosteum in the Brazilian taxon has shown the exact pattern observed in *Europasaurus holgeri* and *Diplodocus* sp.. Our observations indicate that all trabeculae in the

postzygophysis are composed of pneumosteum, corroborating the evidence from the camellate structure. Since derived titanosaurs have demonstrated to be an extreme in pneumaticity (Wedel, 2003; Wedel, 2007; Cerda et al., 2012), this histological result confirms previous hypotheses for the clade (Wedel, 2003; Cerda et al., 2012; Bandeira et al., 2016). However, our results also have shown that pneumosteum is destroyed before complete obliteration of trabeculae in a destructive diagenesis scenario. Therefore, caution is needed when selecting relevant specimens for sampling. Especially when studying stem taxa, one may end up in a false negative absence of pneumosteum in a case where diagenesis had played a destructive role.

5. Conclusions

We presented a new workflow for manipulating CT-scan data to produce photorealistic figure charts using open source multi-system software. The goal is to make this technology more accessible to research groups with limited funding and to potentialize the availability of novel computed tomography paleontological data.

The CT-scan of the cervical vertebra revealed a complex array of smaller cavities that abound inside the centrum and in the postzygophysis. It is possible that the camellate architecture is directly influenced by the air-sacs system that surrounds the vertebra. The posterior cervical CPPLIP-1024 shows a subquadrangular to subtrapezoidal camellate pattern. It may be indicative of the cervical system. This condition differs from the even more chaotic subrounded fabric from the dorsals and caudals of closely related taxa.

We expanded the occurrence of pneumosteum in sauropods to the Brazilian titanosaur *Uberabatitan ribeiroi*. This confirmed previous hypotheses on the insertion of bird-like air sacs system on titanosaurian vertebrae based on external observation and CT-scans. We also highlighted that diagenesis can obliterate traces of pneumosteal bone. One must be cautious to have a good understanding of the diagenetic history of the studied specimen. This could avoid false negatives, especially when sampling pneumatic histological traces in stem taxa.

Acknowledgments

We would like to acknowledge Oswaldo Jorge and the rest of the HU-UFSCar team for conducting fossil tomography. To Arthur Brum for providing insights into pneumosteum. To Filippo Bertozzo for his observations regarding sampling spots. To the anonymous reviewers for their comments. To *Colecionadores de Ossos™* for funding the thin section. Authors research grants, scholarships and financial aid were provided by the Brazilian National Council for Scientific and Technological Development (CNPq) (T.A., T.S.M., and FRB- 303527/2017-0), the Brazilian Coordination for the Improvement of Higher Education Personnel (CAPES) (A.M.G) - Finance Code 001, Fundação de Amparo à Pesquisa do Estado de Minas Gerais (T.S.M.) and FAPESP 2016/20927-0 'Modern accumulation studies and fossil bioclast studies in continental and coastal environments' (F.R.B.) and FAPESP 2018/21094-7 (J.C.G.S.J.).

Fig. 5. Pneumosteum (light yellow arrows) in the posterior cervical vertebra of the titanosaur *Uberabatitan ribeiroi* (CPPLIP-1024). **A**, polished cross-section illustrating sample locations (1–10). Despite bad microstructural preservation, pneumosteal bone still endured diagenesis better in some areas (eg. 1, 3, 4, 6) than the others. Pneumosteum distinguishes from regular primary fibrolamellar and secondary trabecular tissues by presenting an undulose extinction of asbestiform densely-packed fabrics of tiny 'hair-like' fibers. Polarized light under crossed nicols. Scale bar in **A** = 10 mm; in **10** = 20 μ m; in **1, 2, 4–8** = 50 μ m; in **3, 9** = 100 μ m. (For interpretation of the references to colour in this figure legend, the reader is referred to the Web version of this article.)

References

- Aureliano, T., et al., 2018. Semi-aquatic adaptations in a spinosaur from the Lower Cretaceous of Brazil. *Cretaceous Research* 90, 283–295. Available at: <http://www.sciencedirect.com/science/article/pii/S0195667117305153>.
- Bandeira, K.L.N., et al., 2016. A new giant Titanosauria (Dinosauria: Sauropoda) from the Late Cretaceous Bauru Group, Brazil. *PLoS One* 11 (10), e0163373. <https://doi.org/10.1371/journal.pone.0163373>. Available at:
- Bates, K.T., et al., 2010. Sensitivity analysis in evolutionary robotic simulations of bipedal dinosaur running. *Journal of Vertebrate Paleontology* 30 (2), 458–466. <https://doi.org/10.1080/02724630903409329>. Available at:
- Cerda, I.A., Salgado, L., Powell, J.E., 2012. Extreme postcranial pneumaticity in sauropod dinosaurs from South America. *Paläontologische Zeitschrift* 86 (4), 441–449. <https://doi.org/10.1007/s12542-012-0140-6>. Available at:
- Cerda, I.A., et al., 2017. Novel insight into the origin of the growth dynamics of sauropod dinosaurs. *PLoS One* 12 (6), e0179707. <https://doi.org/10.1371/journal.pone.0179707>. Available at:
- CloudCompare, 2018. Version 2.9.1 [GPL software]. Available at: <http://www.cloudcompare.org/>.
- Curry Rogers, K., Kulik, Z., 2018. Osteohistology of *Rapetosaurus krausei* (Sauropoda: Titanosauria) from the Upper Cretaceous of Madagascar. *Journal of Vertebrate Paleontology* 1–24. <https://doi.org/10.1080/02724634.2018.1493689>. Available at:
- da Fonseca Sampaio, L., Dal'Bó, P.F., 2017. Interpretação paleoambiental dos calcetes da Formação Marília na região de Uberaba (MG). *Geologia USP. Série 17* (2), 193–210. Available at: <https://www.revistas.usp.br/guspssc/article/view/134871>.
- Da Mommio, A., 2018. ALEX STREKEISEN: Serpentine. Alex Strekeisen. Available at: <http://www.alexstrekeisen.it/english/meta/serpentine.php>. (Accessed 28 June 2019).
- Dyke, G., et al., 2013. Aerodynamic performance of the feathered dinosaur Micro-raptor and the evolution of feathered flight. *Nature Communications* 4, 2489. <https://doi.org/10.1038/ncomms3489>. Available at:
- Fedorov, A., et al., 2012. 3D Slicer as an image computing platform for the Quantitative Imaging Network. *Magnetic Resonance Imaging* 30 (9), 1323–1341. <https://doi.org/10.1016/j.mri.2012.05.001>. Available at:
- Lambertz, M., Bertozzo, F., Sander, P.M., 2018. Bone histological correlates for air sacs and their implications for understanding the origin of the dinosaurian respiratory system. *Biology Letters* 14 (1). <https://doi.org/10.1098/rsbl.2017.0514>. Available at:
- Lamm, E.-T., 2013. Preparation and Sectioning of Specimens. In: *Bone Histology of Fossil Tetrapods*. University of California Press. Available at: <http://california.universitypressscholarship.com/10.1525/california/9780520273528.001.0001/upso-9780520273528-chapter-4>.
- Mitchell, J., Sander, P.M., 2014. The three-front model: a developmental explanation of long bone diaphyseal histology of Sauropoda. *Biol. J. Linn. Soc. Linn. Soc. Lond.* 112 (4), 765–781. Available at: <https://academic.oup.com/biolinnean/article/112/4/765/2415870>. (Accessed 17 December 2018).
- O'Connor, P.M., 2006. Postcranial pneumaticity: an evaluation of soft-tissue influences on the postcranial skeleton and the reconstruction of pulmonary anatomy in archosaurs. *J. Morphol.* 267 (10), 1199–1226. Available at: <https://onlinelibrary.wiley.com/doi/abs/10.1002/jmor.10470>.
- Padian, K., Lamm, E.-T., 2013. *Bone Histology of Fossil Tetrapods: Advancing Methods, Analysis, and Interpretation*. University of California Press. Available at: <https://market.android.com/details?id=book-EBVNmK1nm6MC>.
- Perry, S.F., et al., 2009. Implications of an avian-style respiratory system for gigantism in sauropod dinosaurs. *Journal of Experimental Zoology. Part A, Ecological Genetics and Physiology* 311 (8), 600–610. Available at: <https://onlinelibrary.wiley.com/doi/abs/10.1002/jez.517>.
- Salgado, L., Carvalho, I.S., 2008. UBERABATITAN RIBEIROI, A NEW TITANOSAUR FROM THE MARÍLIA FORMATION (BAURU GROUP, UPPER CRETACEOUS), MINAS GERAIS, BRAZIL. *Palaeontology*. Available at: <https://onlinelibrary.wiley.com/doi/abs/10.1111/j.1475-4983.2008.00781.x>.
- Sander, P.M., 2013. An evolutionary cascade model for sauropod dinosaur gigantism—overview, update and tests. *PLoS One* 8 (10), e78573. <https://doi.org/10.1371/journal.pone.0078573>. Available at:
- Sander, P.M., et al., 2011. Biology of the sauropod dinosaurs: the evolution of gigantism. *Biological Reviews of the Cambridge Philosophical Society* 86 (1), 117–155. <https://doi.org/10.1111/j.1469-185X.2010.00137.x>. Available at:
- Silva Junior, J.C.G., et al., 2019. Osteology and systematics of *Uberabatitan ribeiroi* (Dinosauria; Sauropoda): a Late Cretaceous titanosaur from Minas Gerais, Brazil. *Zootaxa* 4577 (3), 401–438. Available at: https://www.researchgate.net/profile/Julian_Silva_Junior/publication/332274953_Osteology_and_systematics_of_Uberabatitan_ribeiroi_Dinosauria_Sauropoda_a_Late_Cretaceous_titanosaur_from_Minas_Gerais_Brazil/links/5cab507d92851c64bd581393/Osteology-and-systematics-of-Uberabatitan-ribeiroi-Dinosauria-Sauropoda-a-Late-Cretaceous-titanosaur-from-Minas-Gerais-Brazil.pdf.
- Tarini, M., Cignoni, P., Scopigno, R., 2003. Visibility Based Methods and Assessment for Detail-recovery. In: *Proceedings of the 14th IEEE Visualization 2003 (VIS'03)*. VIS '03. IEEE Computer Society, Washington, DC, USA, p. 60. <https://doi.org/10.1109/VISUAL.2003.1250407>. Available at:
- Wedel, M.J., 2003. Vertebral pneumaticity, air sacs, and the physiology of sauropod dinosaurs. *Paleobiology* 29 (2), 243–255. Available at: <https://www.cambridge.org/core/journals/paleobiology/article/vertebral-pneumaticity-air-sacs-and-the-physiology-of-sauropod-dinosaurs/22C8C9E2378D8DCCD32BE689459EF620>. (Accessed 20 June 2019).
- Wedel, M.J., 2006. Origin of postcranial skeletal pneumaticity in dinosaurs. *Integrative Zoology* 1 (2), 80–85. <https://doi.org/10.1111/j.1749-4877.2006.00019.x>. Available at:
- Wedel, M.J., 2007. What pneumaticity tells us about “prosaurotops”, and vice versa. *Special Papers in Palaeontology* 77, 207–222. Available at: https://www.researchgate.net/profile/Mathew_Wedel/publication/272152712_What_pneumaticity_tells_us_about_prosaurotops%E2%80%99and_vice-versa/links/57d2e0e108ae5f03b48cd10c/What-pneumaticity-tells-us-about-prosaurotops-and-vice-versa.pdf.
- Wedel, M.J., 2009. Evidence for bird-like air sacs in saurischian dinosaurs. *Journal of Experimental Zoology. Part A, Ecological Genetics and Physiology* 311 (8), 611–628. Available at: <https://onlinelibrary.wiley.com/doi/abs/10.1002/jez.513>.
- Wedel, M.J., Cifelli, R.L., Sanders, R.K., 2000. Osteology, paleobiology, and relationships of the sauropod dinosaur *Sauroposeidon*. *Acta Palaeontologica Polonica* 45 (4).
- Wilson, J.A., 2012. New vertebral laminae and patterns of serial variation in vertebral laminae of sauropod dinosaurs. Available at: <https://deepblue.lib.umich.edu/bitstream/handle/2027.42/92460/Contributions32no7-HR-c08-15-2012.pdf?sequence=2>.
- Wilson, J.A., et al., 2011. A nomenclature for vertebral fossae in sauropods and other saurischian dinosaurs. *PLoS One* 6 (2), e17114. <https://doi.org/10.1371/journal.pone.0017114>. Available at:
- Xu, X., et al., 2015. A bizarre Jurassic maniraptoran theropod with preserved evidence of membranous wings. *Nature* 521 (7550), 70–73. <https://doi.org/10.1038/nature14423>. Available at:
- Yates, A.M., Wedel, M.J., Bannan, M.F., 2012. The early evolution of postcranial skeletal pneumaticity in sauropodomorph dinosaurs. *Acta Palaeontologica Polonica* 57 (1), 85–100. Available at: <http://www.app.pan.pl/article/item/app20100075.html>.